Proc. Estonian Acad. Sci. Engng., 1998, **4**, 4, 286–306
https://doi.org/10.3176/eng.1998.4.03

CYCLIC FATIGUE EVALUATION IN METALS UNDER RANDOM OSCILLATING STRESSES

Ivan KLEVTSOV[a] and Roger CRANE[b]

[a] Institute of Thermal Engineering, Tallinn Technical University, Kopli 116, 11712 Tallinn, Estonia; e-mail: klevtsov@sti.ttu.ee
[b] Department of Mechanical Engineering, University of South Florida, 4202 Fowler Avenue, Tampa, Florida 33620-5350, USA; e-mail: crane@eng.usf.edu

Received 20 March 1998

Abstract. A direct modelling method was developed to improve the accuracy of metal fatigue life estimates. The procedures were developed for the evaluation of once-through steam generator tubes, however, intended to be generally applicable. Random thermal boundary conditions were first simulated, with specific consideration given to the cases of transition boiling and fluctuating coolant inlet temperatures. Subsequently, transient heat transfer rates were determined, and wall stresses due to pressure and temperature oscillations were calculated. The resultant wall temperature and stress oscillation data were statistically analyzed to provide the effective parameters used to estimate the metal fatigue.

Key words: once-through steam generator, transition boiling, thermal stress, cyclic fatigue, fatigue life prediction.

NOMENCLATURE

A	amplitude		
C_τ	maximum time fluctuation	α	thermal expansion coefficient
c	tube metal specific heat	β	Biot number
E	modulus of elasticity	δ	limiting parameter
f	frequency	θ	fluctuation period
$G(k)$	spectral density	ν	Poisson's ratio
h	convective coefficient	ρ	density of the tube metal
k	metal thermal conductivity	σ	stress
K_f	frequency transmission coefficient	σ_{-1}	fatigue endurance limit
$K_{s,f}$	stress transmission coefficient	τ	time or time interval
l	length of the rivulet		
l_{rel}	relative length of the rivulet		

L_{max}	maximum amplitude of transition zone fluctuations
m	time interval number
N	cycle number
N_0	basic cycle number
n	point number
P	pressure
p	probability
R_1	outside radius of the tube
R_2	inside radius of the tube
$R(\tau)$	autocorrelation function
r	radial coordinate
S	intensity of oscillations
T	temperature
V	autocorrelation exponent

Subscripts

1	hot side
2	cold side
eq	equivalent
f	film boiling condition
m	mean
t	temperature

1. INTRODUCTION

The determination of effects of thermal stress oscillations on fatigue damage continues to be topical. Stress calculation methods have generally followed one of the two approaches. The first approach [1] is based on an analytical solution of the energy and elasticity equations as applied to stress fields with random oscillating boundary conditions. The second uses a numerical computation model [2,3] to provide a more detailed treatment of the basic problem and associated boundary conditions. Up to now, numerical solutions have been obtained only for harmonic oscillations. Transition boiling, characterized by a combination of high frequency rivulet fluctuations and low frequency zone fluctuations associated with hydrodynamic instabilities, will require a refined treatment. The basic problem is sufficiently complex to warrant a detailed investigation without oversimplifying the model or the boundary conditions. Such a study is considered to be most amenable to numerical methods.

Like the thermal stress oscillations, fatigue life estimation methods may also be analytical or numerical. An analytical method has been developed [1], based on the correlation theory of random processes. The method assumes a continuous Gaussian distribution of the stresses and a limiting Rayleigh distribution of stress amplitudes. Using the linear cumulative damage rule, a simple equation for fatigue life estimation has been obtained. A numerical computation, using the double-linear damage rule concept for fatigue life estimation with discrete or continuous distribution of loading curve amplitudes [4], has also been completed. As reported previously [5], the differences between the two estimates are negligible when stress amplitudes may be accurately represented by a continuous Rayleigh distribution, but diverge as the fit degrades.

A primary purpose of this work is to develop a computational program for direct modelling of stress oscillations induced by random fluctuations of

boundary conditions. Subsequently, a more accurate estimate of material fatigue life will be established. The specific application selected for this purpose is an once-through steam generator tube, shown in Fig. 1. Under normal operating conditions, random oscillations will occur in the heat transfer conditions in the liquid-vapour interface and at the convective interface itself.

2. COMPUTATION MODEL

Random boundary conditions are initially established. The two cases considered are: 1) transient convective coefficients which are effective in the transition boiling zone of an once-through steam generator, and 2) transient fluid inlet temperature occurs in a direct contact heat exchanger. Using a random number generator, a matrix of heat transfer coefficients or fluid inlet temperatures, with appropriate random time coordinates, are developed:

$$h_2(n) = (h_n - h_f) \cdot RND(n) + h_f,$$

$$\tau(n) = \tau(n-1) \cdot RND(n) \cdot C_\tau.$$

These conditions are then transformed to constant time increments by the interpolation of the random time interval data.

The governing one dimensional energy equation may be written as

$$\rho c \frac{\partial T}{\partial \tau} = \frac{1}{r} \frac{\partial}{\partial r} \left(kr \frac{\partial T}{\partial r} \right),$$

where the boundary conditions are given by

$$-k \left. \frac{\partial T}{\partial r} \right|_{r=R_1} = h_1 [T(R_1, \tau) - T_1],$$

$$-k \left. \frac{\partial T}{\partial r} \right|_{r=R_2} = h_2 [T(R_2, \tau) - T_2].$$

The conditions of transition boiling have been simulated assuming that the inside coolant temperature T_2 is constant and that the associated convective transition coefficient h_2 is a random function of time. Alternately, when simulating, h_2 is assumed constant, and T_2 is assumed to be a random function of time. In both cases h_1 and T_1 are generally taken as constants. In a limited number of cases perturbation of h_1 and T_1 was considered, to determine the effect of the hot side Biot number. The Crank–Nicolson semi-implicit transient finite difference algorithm has been used to solve the resultant energy equation.

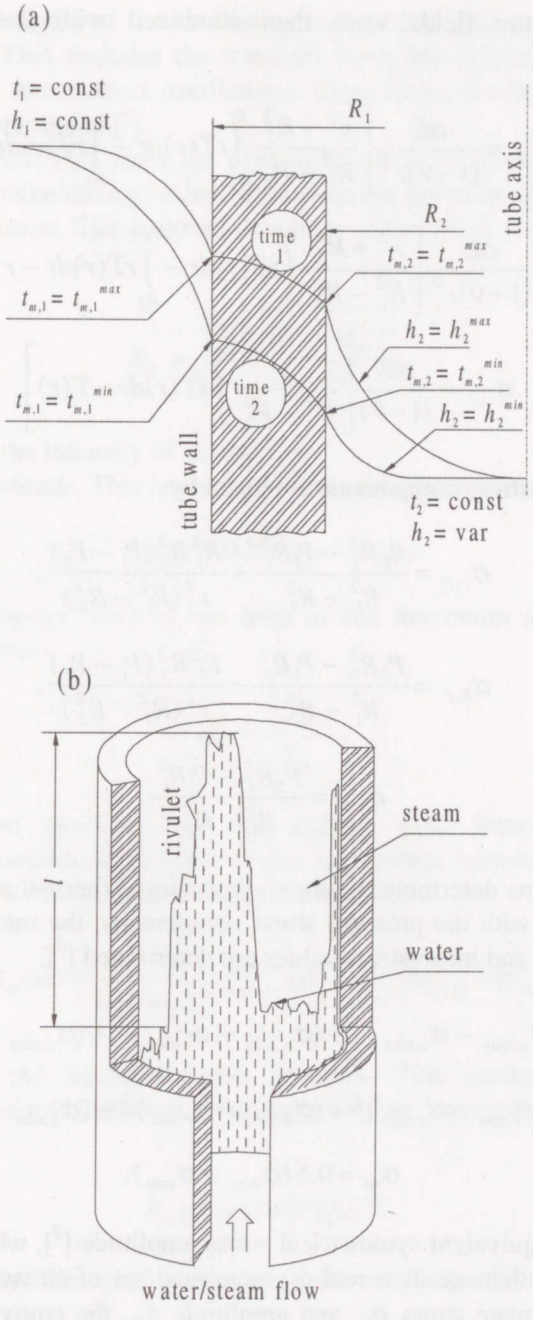

Fig. 1. Fluid flow (a) and heat transfer (b) in the transition boiling zone of the once-through steam generator.

The temperature fields were then combined with the thermoelasticity equations

$$\sigma_{r,T} = \frac{\alpha E}{(1-\nu)r^2}\left[\frac{r^2+R_2^2}{R_1^2-R_2^2}\int_{R_2}^{R_1} rT(r)dr - \int_{R_2}^{r} rT(r)dr\right],$$

$$\sigma_{\theta,T} = \frac{\alpha E}{(1-\nu)r^2}\left[\frac{r^2+R_2^2}{R_1^2-R_2^2}\int_{R_2}^{R_1} rT(r)dr - \int_{R_2}^{r} rT(r)dr - r^2T(r)\right],$$

$$\sigma_{z,T} = \frac{\alpha E}{(1-\nu)}\left[\frac{2}{R_1^2-R_2^2}\int_{R_2}^{R_1} rT(r)dr - T(r)\right].$$

Pressure induced stress components are given by

$$\sigma_{r,P} = \frac{P_2R_2^2 - P_1R_1^2}{R_1^2-R_2^2} + \frac{R_1^2R_2^2(P_1-P_2)}{r^2(R_1^2-R_2^2)},$$

$$\sigma_{\theta,P} = \frac{P_2R_2^2 - P_1R_1^2}{R_1^2-R_2^2} - \frac{R_1^2R_2^2(P_1-P_2)}{r^2(R_1^2-R_2^2)},$$

$$\sigma_{z,P} = \frac{P_2R_2^2 - P_1R_1^2}{R_1^2-R_2^2}.$$

These equations determine the three dimensional thermal stress components. When combined with the pressure stress components, the maximum oscillating stress amplitudes and mean stress values are determined [6]:

$$\sigma_{\max} = \left\{0.5\left[(\sigma_{r,\max}-\sigma_{z,\max})^2 + (\sigma_{\theta,\max}-\sigma_{r,\max})^2 + (\sigma_{z,\max}-\sigma_{\theta,\max})^2\right]\right\}^{0.5},$$

$$\sigma_{\min} = \left\{0.5\left[(\sigma_{r,\min}-\sigma_{z,\min})^2 + (\sigma_{\theta,\min}-\sigma_{r,\min})^2 + (\sigma_{z,\min}-\sigma_{\theta,\min})^2\right]\right\}^{0.5},$$

$$\sigma_m = 0.5\,(\sigma_{\max} + \sigma_{\min}).$$

Defining an equivalent symmetrical stress amplitude [7], which would induce the same fatigue damage as a real asymmetrical set of stresses having a mean value σ_m, an ultimate stress σ_u, and amplitude A_σ, the equivalent symmetrical stress is given as

$$A_{\sigma,eq} = \frac{A_\sigma}{1-\sigma_m/\sigma_u}.$$

A statistical analysis of the oscillating temperature and stress parameters is then performed. This includes the transient boundary conditions, tube surface temperatures and metal stress oscillations. From these, the following statistical parameters are determined [8].

Arithmetic mean. This fixes the asymmetry of the loading and is used, for example, to determine the equivalent stresses in the previous equation.

Standard deviation. The standard deviation of the stress values is determined as

$$S_\sigma = \sqrt{\frac{\sum_{i=1}^{n} (\sigma_i - \sigma_\mathrm{m})^2}{(n-1)}},$$

and is defined as the intensity of oscillations.

Maximum amplitude. This is one half of the maximum observed stress range

$$A_{\sigma,\max} = 0.5(\sigma_{\max} - \sigma_{\min}).$$

Limiting parameter. This is the ratio of the maximum amplitude and the oscillation intensity:

$$\delta_\sigma = \frac{A_{\sigma,\max}}{S_\sigma}.$$

Autocorrelation function. For the current time interval $\tau = m\Delta\tau$, the autocorrelation function is defined as the correlation between two oscillation curve ordinates over the corresponding time interval

$$R_\sigma(m) = \frac{1}{(n-m)S_\sigma^2} \sum_{i=1}^{n-m} (\sigma_i - \sigma_\mathrm{m})(\sigma_{i+m} - \sigma_\mathrm{m}).$$

Exponent of the autocorrelation function. This parameter is used to approximate the autocorrelation function using an equation of the following form [1]:

$$R_\sigma(\tau) = (1 + |V\tau|)e^{-V\tau}.$$

Spectral density. The spectral density of the oscillation distribution is defined as

$$G_\sigma(k) = 2\Delta\tau \left[R_\sigma(0) + 2\sum_{m=1}^{n-1} D_m R_\sigma(m) \cos\left(\frac{\pi m k}{n}\right) \right],$$

where

$$D_m = \left[1 + \cos\left(\frac{\pi m}{n}\right)\right] \quad \text{for} \quad m = 0, 1, 2...n,$$

$$D_m = 0 \quad \text{for} \quad m > n.$$

Effective oscillation period. The effective period is

$$\theta_{\sigma,\text{ef}} = \left[\frac{\sum_{i=0}^{n} G_\sigma(i)}{\sum_{i=0}^{n} G_\sigma(i) f_i^2}\right]^{0.5},$$

where the frequency of the current is defined as $f_i = i/(2n\Delta\tau)$.

The transmission coefficient of oscillation intensity is defined as

$$K_s = \frac{1-\nu}{\alpha E}\frac{S_\sigma}{S_t},$$

and the frequency transmission coefficient as

$$K_f = \frac{f_\sigma}{f_t} = \frac{\theta_t}{\theta_\sigma}.$$

The basic parameters to be evaluated statistically include the transient heat transfer coefficient, metal surface temperature and surface stresses [5]. All the stress parameters are evaluated first for the constant time interval simulation and second for the oscillation amplitudes determined using the range pair method of cycle estimation [7]. Results from the first evaluation are termed as being "stress value based" and from the second being "stress amplitude based". In the latter case, the effective period of the cycle has been taken as the total process time divided by the number of effective cycles.

By evaluating these results, the double-linear rule has been used to estimate metal fatigue life [4]. Distributions of the probability of the stress amplitude were determined from the statistical analysis of the loading curve. For the "stress value based" case, equivalent amplitudes have been obtained by adapting the asymmetrical amplitudes to the mean values for the entire process. For the "stress amplitude based" case, equivalent amplitudes have been determined for each step to account for variations in the mean stress.

3. COMPUTATIONAL RESULTS

The wall temperature and thermal stress oscillations may be induced by two types of boundary conditions. The first is typical for transition boiling with convective coefficients which alternate between nucleate and film boiling. The

second, which is typical for direct contact heat exchangers, is represented by sudden changes in the fluid inlet temperature. Both cases have been examined to determine the influence of the Biot number. The departure from nucleate boiling or transition boiling zone of a once-through steam generator helical coiled tube was selected for testing in this investigation. The design and operating parameters are shown in Table 1.

Table 1

Basic design and operating parameters

Parameter	Value
Outside diameter of the tube, mm	22
Tube wall thickness, mm	3
Coil diameter, mm	110
Coefficient of thermal expansion $\times 10^6$, K^{-1}	12.1
Modulus of elasticity $\times 10^{-5}$, MPa	2.1
Poisson's ratio	0.4
Fatigue endurance limit, MPa	80
Thermal conductivity, $W/(m \cdot K)$	35.1
Water/steam pressure, MPa	10
Saturation temperature, °C	310.4
Nucleate boiling heat transfer coefficient, $kW/(m^2 \cdot K)$	97.7
Film boiling heat transfer coefficient, $kW/(m^2 \cdot K)$	5.41
Heated fluid (helium) pressure, MPa	4
Heated fluid temperature, °C	641.5
Heated fluid heat transfer coefficient, $kW/(m^2 \cdot K)$	1.48

A limited number of cases have been considered in addition to determine the influence of the hot side Biot number. Operating parameters were selected so that the tube surface temperature variations on the cold side corresponded to those in Table 1, but hot side flow convective coefficients were extended to include also gases, pressurized water and liquid metals. Cold side flow variations provided a range of cold wall conditions from steady nucleate boiling to steady film boiling. Operating parameters for these cases are shown in Table 2.

Within a once-through steam generator, both high and low frequency oscillations occur. The liquid film covering the tube wall perimeter will occasionally break off, forming rivulets interspaced by dry patches. The difference between the heat transfer coefficients from wall to water (nucleate boiling) and from wall to vapour (film boiling) produces oscillations in the tube wall temperature and, consequently, in the thermal stresses. These oscillations occur with relatively high frequency, producing oscillations of about 1 Hz. This type of high frequency oscillation is shown in Fig. 2.

Table 2

Extended operating conditions to evaluate effects of Biot number

Cold side convective coefficient pulsations

Hot side			Cold side					
Temperature, °C	Convective coefficient, $kW \cdot m^{-2} \cdot K^{-1}$	Biot number	Temperature, °C	Convective coefficient, $kW \cdot m^{-2} \cdot K^{-1}$		Biot number		
				max	min	max	min	mean
641.5	1.48	0.126	260	10.2	3.3	0.87	0.29	0.58
			301.7	39.4	4.9	3.4	0.42	1.91
			310.4	97.7	5.4	8.35	0.46	4.4
			313.2	187	5.6	16	0.48	8.24
471	7	0.6	243	11.9	3	1.02	0.26	0.64
			294	39.4	4.55	3.4	0.39	1.9
			307	97.7	5.3	8.35	0.45	4.4
			312	187	5.6	16	0.47	8.24
434	33.5	2.86	191	10	2.2	0.85	0.19	0.52
			286	41	4.2	3.5	0.36	1.93
			304	97.7	5	8.35	0.43	4.4
			310	187	5.4	16	0.46	8.24

Cold side inlet temperature pulsations

Hot side			Cold side			
Temperature, °C	Convective coefficient, $kW \cdot m^{-2} \cdot K^{-1}$	Biot number	Convective coefficient, $kW \cdot m^{-2} \cdot K^{-1}$	Biot number	Temperature, °C	
					max	min
641.5	1.48	0.126	5.41	0.46	310.4	209.8
			23	1.97	372.9	291.2
			51.6	4.4	383.5	305.1
			97.7	8.35	387.6	310.4
471	7	0.6	5.41	0.46	309.5	154.4
			23	1.97	372.7	278.2
			51.6	4.4	383.4	299.3
			97.7	8.35	387.5	307.3
434	33.5	2.86	5.41	0.46	310.4	85.7
			23	1.97	372.8	262
			51.6	4.4	383.5	292.1
			97.7	8.35	387.6	303.5

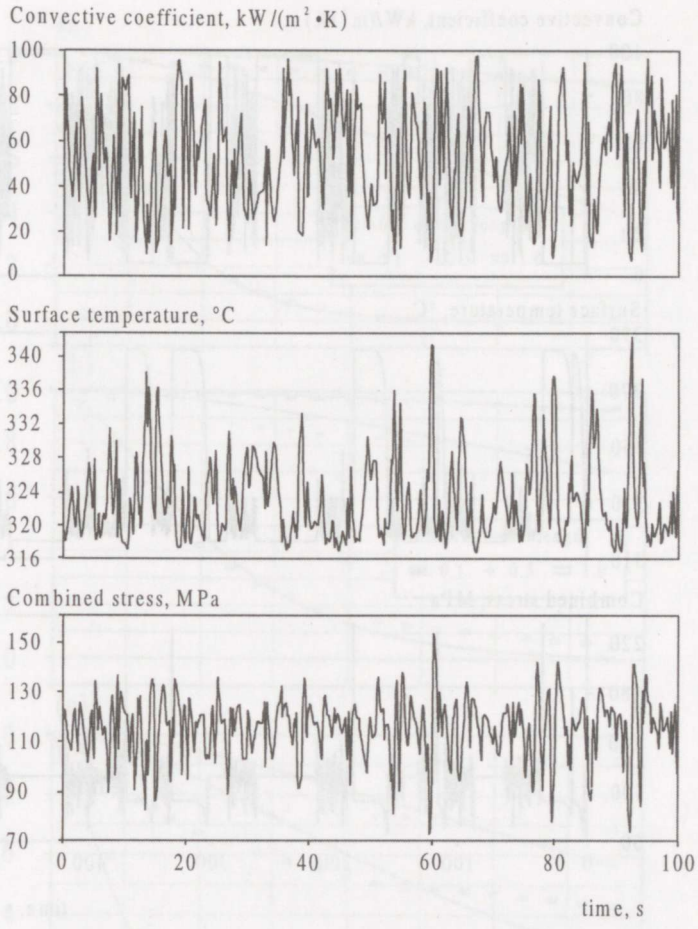

Fig. 2. Materials response to high frequency random thermal oscillations.

Simultaneously, the transition boiling zone itself shifts up and down along the tube axis due to hydraulic instability. Those low frequency fluctuations, producing oscillations of about 1/60 Hz, lead to combined temperature and stress oscillations, shown in Fig. 3, and are described using the relative rivulet length parameter as

$$l_{\text{rel}} = \frac{l}{(2L_{\max})}.$$

The maximum rivulet length depends on several parameters, but is found to be about 80 mm for straight evaporator tubes and about 300 mm for helical coiled tubes. Since the fluctuation amplitudes induced by hydraulic instabilities are highly variable, the relative rivulet length was selected as a free parameter. For $l_{\text{rel}} \geq 1$, the whole tube perimeter is subjected to high frequency oscillations

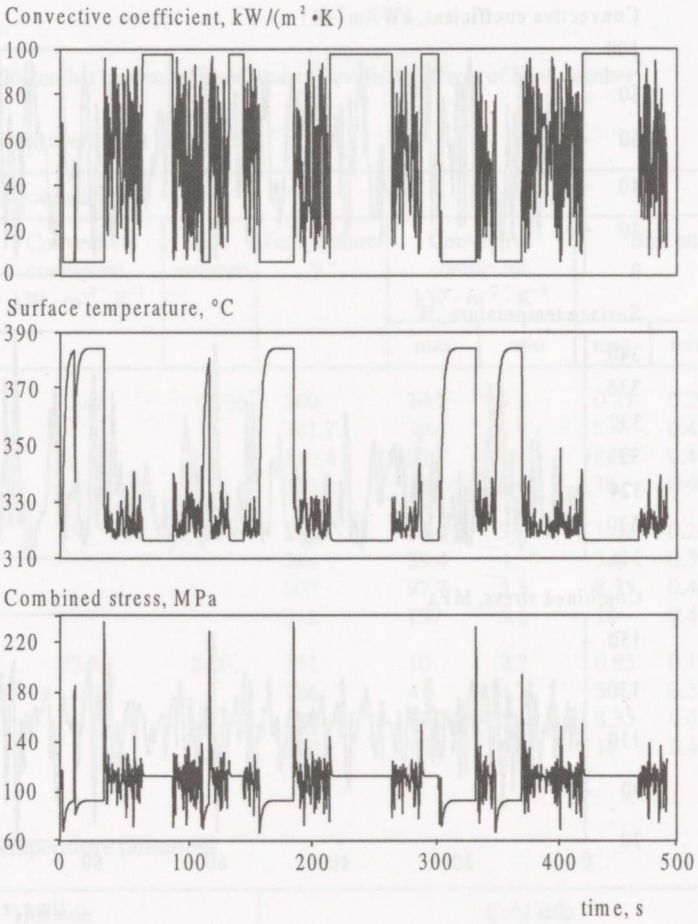

Fig. 3. Response to combined high and low frequency random thermal oscillations.

due to the alternate formation of rivulets and dry patches. For $l_{rel} < 1$, the tube perimeter will be subjected to either liquid or vapour, interrupted occasionally by the alternate formation of dry patches or rivulets. Assuming these boundary conditions, direct solution of the hydraulic instability problem is obtained; results are shown in Fig. 3.

4. STATISTICAL PARAMETERS OF OSCILLATION

Data for the autocorrelation functions have been approximated from the statistical analysis of the simulation data, using exponential equations. The data are shown in Fig. 4 together with the approximations (solid curves). This allows the determination of the autocorrelation exponent V, used as the basic parameter for the evaluation of the transmission oefficient. The exponent type equation

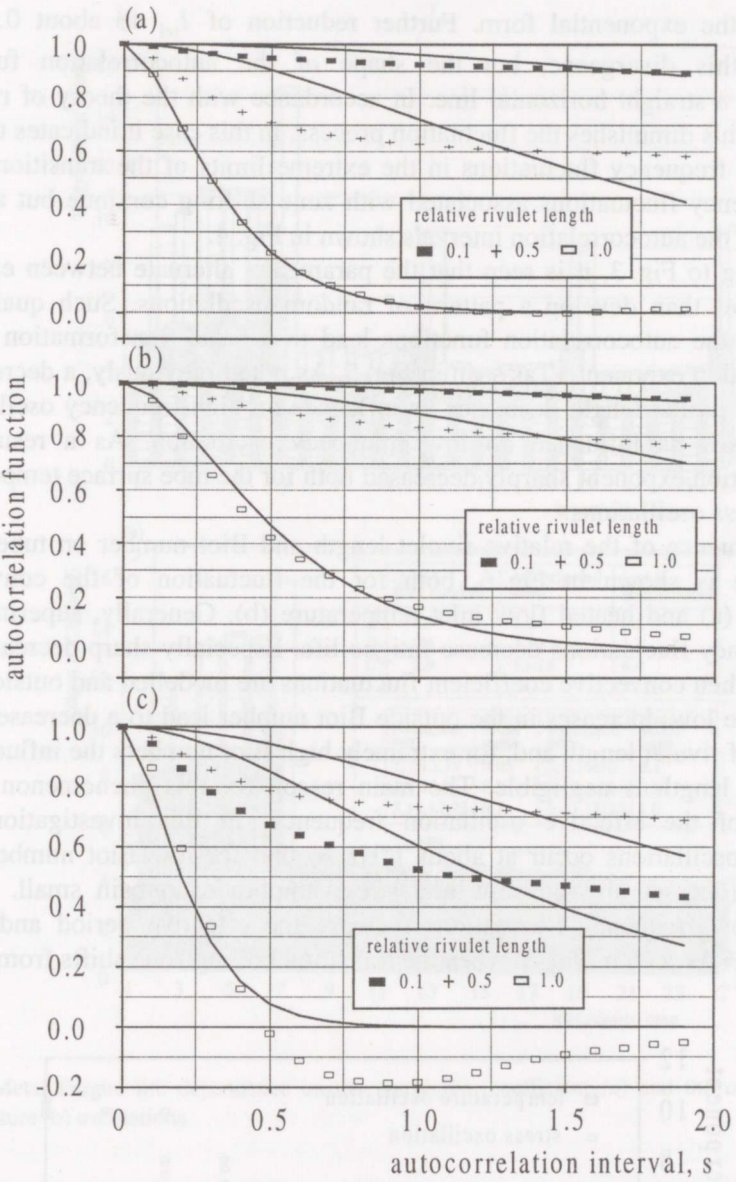

Fig. 4. Autocorrelation functions for the convective coefficient (a), temperature (b) and stress (c) oscillations, depending on the relative rivulet length and the autocorrelation interval; approximations are shown by solid curves.

yields a relatively accurate approximation in the case of high frequency oscillations, as seen in cases when $l_{rel} \approx 1$. In these cases, data appear to follow approximately Gaussian type distribution. Superimposed low frequency fluctuations decrease l_{rel} to about 0.5 and lead to a significant divergence of the

data from the exponential form. Further reduction of l_{rel} to about 0.1 also decreases this divergence, but the shape of the autocorrelation function approaches a straight horizontal line. In accordance with the theory of random processes, this diminishes the fluctuation process. In this case it indicates the end of the high frequency fluctuations in the extreme limits of the transition zone. Low frequency fluctuations associated with zone shifting continue but are not reflected in the autocorrelation intervals shown in Fig. 4.

Referring to Fig. 3, it is seen that the parameters alternate between extreme values rather than develop a pattern of random oscillations. Such qualitative changes of the autocorrelation functions lead to a basic transformation in the autocorrelation exponent V, as seen in Fig. 5. As noted previously, a decrease of the relative rivulet length decreases its influence on high frequency oscillations and increases its influence on low frequency oscillation. As a result, the autocorrelation exponent sharply decreased both for the tube surface temperature and the stress oscillations.

The influence of the relative rivulet length and Biot number on tube metal fatigue life is shown in Fig. 6, both for the fluctuation of the convective coefficient (a) and heated flow inlet temperature (b). Generally, superimposed low frequency fluctuations decrease fatigue life. Especially sharp decreases are observed when convective coefficient fluctuations are modelled and outside Biot numbers are low. Increases in the outside Biot number lead to a decrease in the influence of rivulet length and, for extremely high Biot numbers the influence of the rivulet length is negligible. The main reason for this phenomenon is the influence of the effective oscillation frequency. In this investigation high frequency oscillations occur at about 1 Hz so that for low Biot numbers, the transient processes are too slow and stress amplitudes remain small. Superimposed low frequency fluctuations increase the effective period and stress amplitudes. As seen in Fig. 3, when the transition boiling zone shifts from liquid

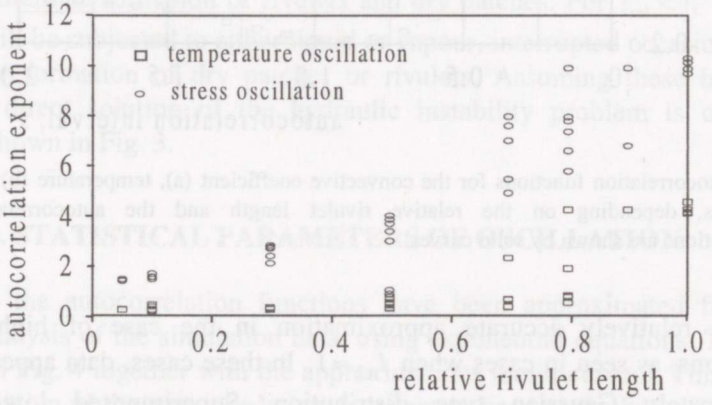

Fig. 5. Approximation of the autocorrelation functions.

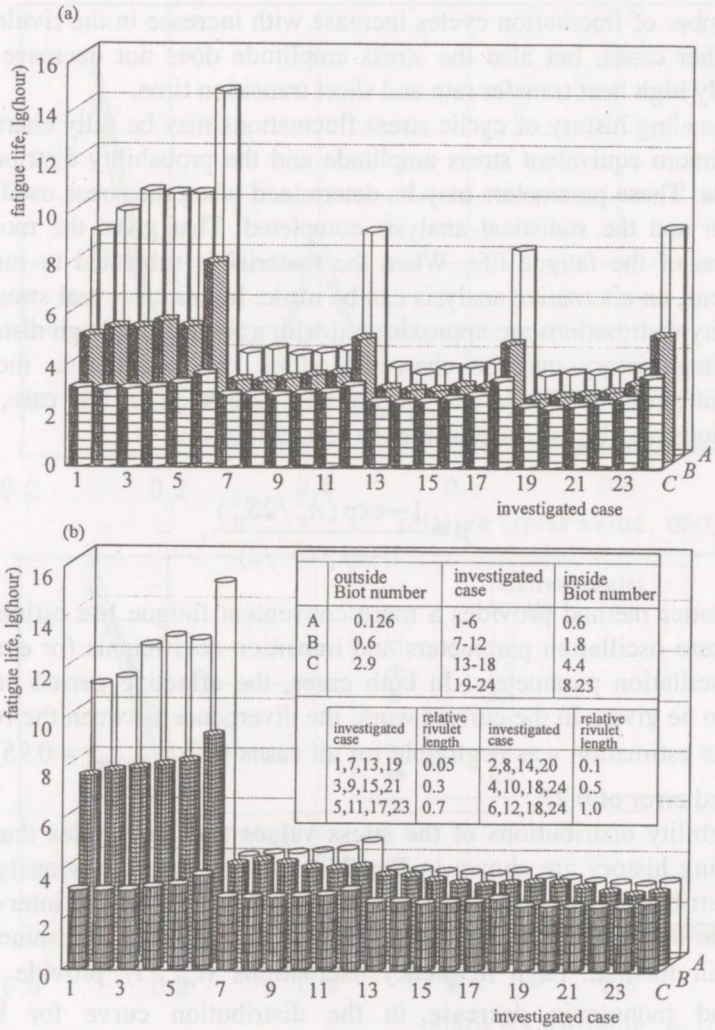

	outside Biot number	investigated case	inside Biot number
A	0.126	1-6	0.6
B	0.6	7-12	1.8
C	2.9	13-18	4.4
		19-24	8.23

investigated case	relative rivulet length	investigated case	relative rivulet length
1,7,13,19	0.05	2,8,14,20	0.1
3,9,15,21	0.3	4,10,18,24	0.5
5,11,17,23	0.7	6,12,18,24	1.0

Fig. 6. Metal fatigue life dependence on the convective coefficient (a) and the cold flow inlet temperature (b) oscillations.

to vapour, the tube surface is covered with steam and the heat transfer rate becomes quite low. When this zone shifts back from vapour to liquid, the superheated metal undergoes high heat fluxes with intensive nucleate boiling. This leads to a sharp decrease in tube wall temperature, a sudden increase in stress due to thermal shock and a significant decrease in fatigue life. For the cases when the flow inlet temperature fluctuations are modelled, similar significant variations of fatigue life with rivulet length are not observed. For extremely high Biot numbers, the fatigue life continuously decreases with the increase in the rivulet length. This phenomenon occurs because not only does the

total number of fluctuation cycles increase with increase in the rivulet length, as in all other cases, but also the stress amplitude does not decrease due to the constantly high heat transfer rate and short transition time.

The loading history of cyclic stress fluctuations may be fully characterized by the maximum equivalent stress amplitude and the probability distribution of the amplitude. These parameters may be determined when the stress oscillation curve is known and the statistical analysis completed. That gives the most complete estimation of the fatigue life. When the material is subjected to random stress oscillations, an alternative analysis can be made. In this case, real stress amplitude probability distributions are approximated with a limited Rayleigh distribution and the loading history may be characterized by two parameters: the maximum equivalent stress amplitude and the limiting parameter. In this case, probability distributions may be estimated using the equation

$$p = \frac{1 - \exp\left(A_\sigma^2 / 2S_\sigma^2\right)}{1 - \exp\left(\delta^2 / 2\right)}.$$

The latter method provides a more convenient fatigue life estimation, using temperature oscillation parameters and transition coefficients for evaluating the stress oscillation parameters. In both cases, the effective period of pulsations must also be given. In the current work, the divergence between the two methods of fatigue estimation was negligible for all cases with $\tau_{\text{Rayleigh}} = 0.95\,\tau_{\text{initial}}$, with a standard error of 0.27.

Probability distributions of the stress values and amplitudes that determine the loading history are shown in Fig. 7. As it was noted previously, the stress value distribution was calculated on the basis of constant time intervals and the amplitude distribution on the basis of rows of amplitudes determined using the range pair method. High frequency oscillations ($l_{\text{rel}} \geq 1$) provide a relatively slow and monotonic decrease in the distribution curve for both cases, approaching normal Gaussian or Rayleigh distribution. The superposition of low frequency oscillations leads to a sharp growth of the rate of low stresses in the loading history so that about 60% of the stress data do not exceed 10% of the maximum value. The amplitudes monotonically decrease with an increase of the relative amplitude. The stress value has a significant peak at 0.4–0.5, corresponding to the condition of stable nucleate boiling. It was found that, despite the significant divergence in the distributions and in the effective period, the divergence between "stress value based" and "amplitude based" fatigue life estimations is also negligible (Fig. 8). It was found that $\tau_{\text{str}} = 0.983\,\tau_{\text{ampl}}$ with a standard error of 0.432. Consequently, accurate fatigue life estimation may use an "stress value based" stress oscillation intensity, limiting parameter, and effective period. These may be evaluated from the surface temperature oscillation curve and transmission coefficients.

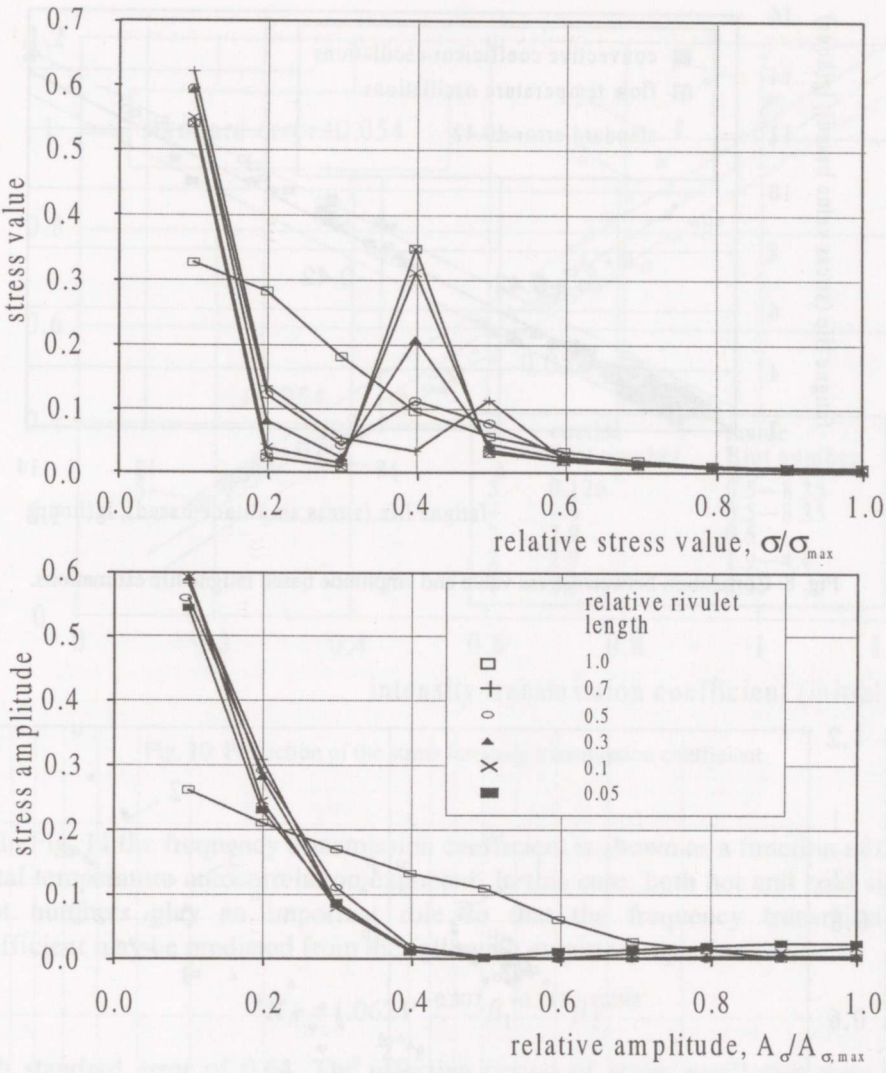

Fig. 7. Stress value and amplitude probability distributions.

In Fig. 9, the stress oscillation intensity transmission coefficient is shown as a function of the autocorrelation exponent of surface temperature oscillation. In Fig. 10, the predicted coefficients are presented in comparison with their initial values. Biot numbers correspond to convective coefficients on the hot and cold sides. The hot side Biot numbers are seen to have a strong influence on stress intensity while the cold side effects are negligible. In addition, the auto-correlation exponent V has a strong influence on the stress intensity so that the oscillation intensity transmission coefficient may be described as

$$K_s = 0.425 + 0.134 \cdot \beta_1 + 0.431 \cdot \lg V_t$$

with a standard error of 0.055. Here β_1 is approximation coefficient.

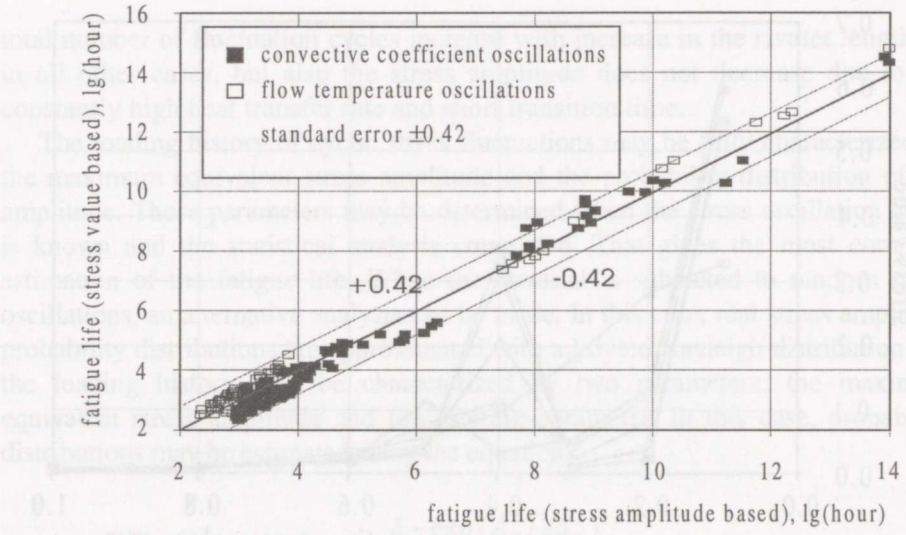

Fig. 8. Correlation between stress value and amplitude based fatigue life estimations.

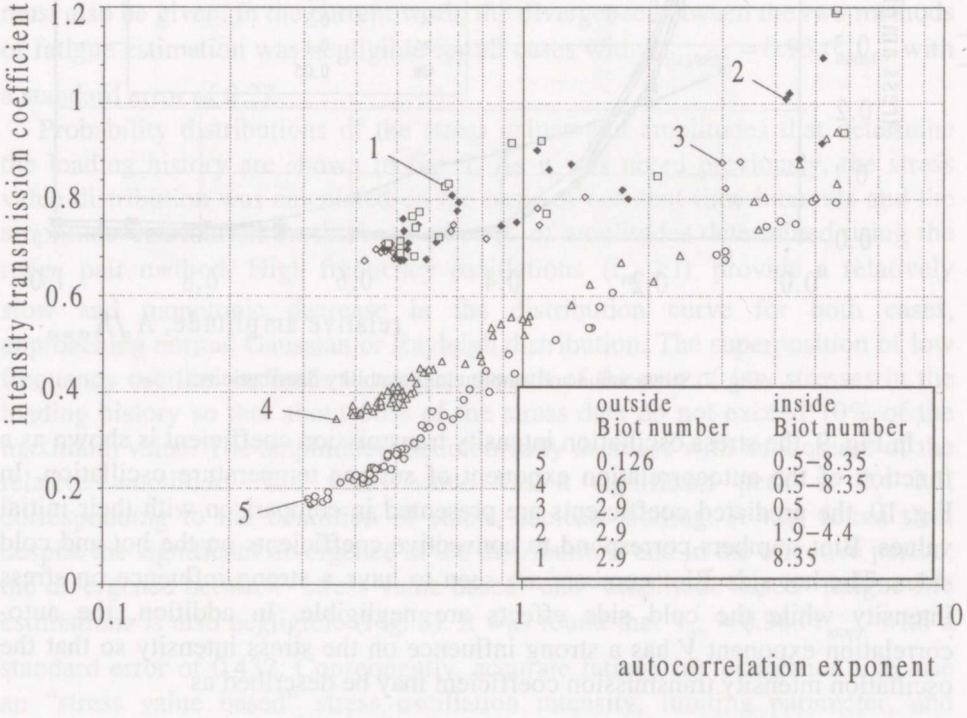

Fig. 9. Stress oscillation intensity transmission coefficient.

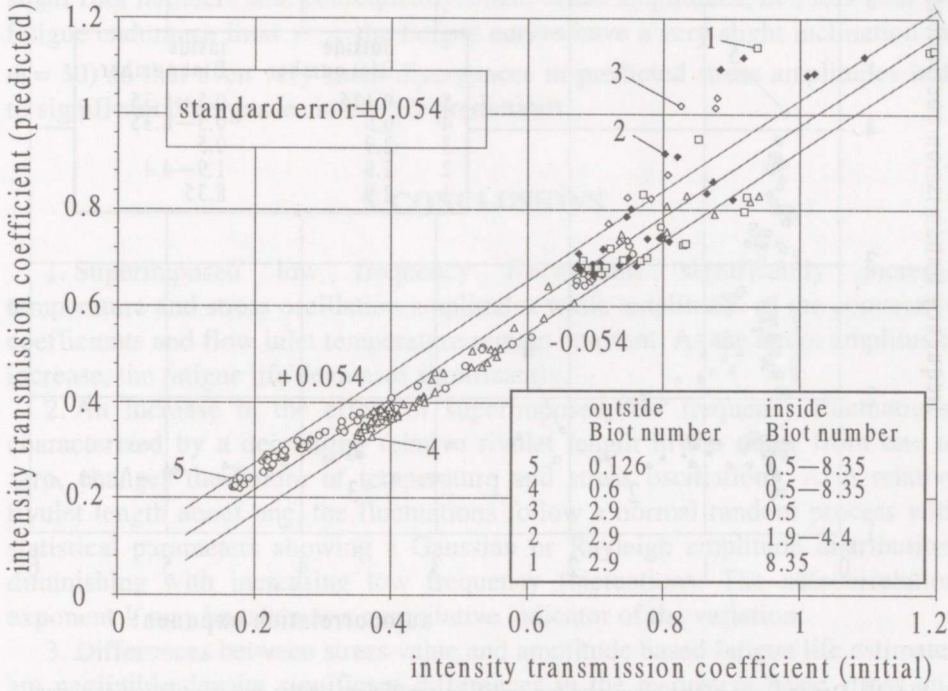

Fig. 10. Prediction of the stress intensity transmission coefficient.

In Fig. 11 the frequency transmission coefficient is shown as a function of the metal temperature autocorrelation exponent. In this case, both hot and cold side Biot numbers play an important role so that the frequency transmission coefficient may be predicted from the following empirical equation:

$$K_\delta = 1.062 V^{-0.307} \beta_1^{-0.157} \beta_2^{0.299},$$

with standard error of 0.64. The effective period of stress oscillation may be approximated by the following empirical equation

$$\lg K_f = 0.489 - 0.0561 \lg \beta_1 - 0.498 \lg V - 1.498 \left[\exp(0.1 \beta_1^{0.25} / V) - 1\right],$$

with a standard error of 0.305. Predictions of stress oscillation parameters were completed using surface temperature oscillation data. Predictions of fatigue life incorporated the stress oscillation parameters and a limiting Rayleigh type amplitude probability distribution. Comparisons with the initial life estimations are shown in Fig. 12. Life predictions based on this method are seen to be rather conservative with $\tau_{pred} = 0.86\ \tau_{init}$ with a standard error of 1.1. The greatest divergence takes place where the minimum Biot numbers occur. This is attributed to the shape of the fatigue curve, given as $N = N_0 (\sigma_{-1} / A_\sigma)^m$. For

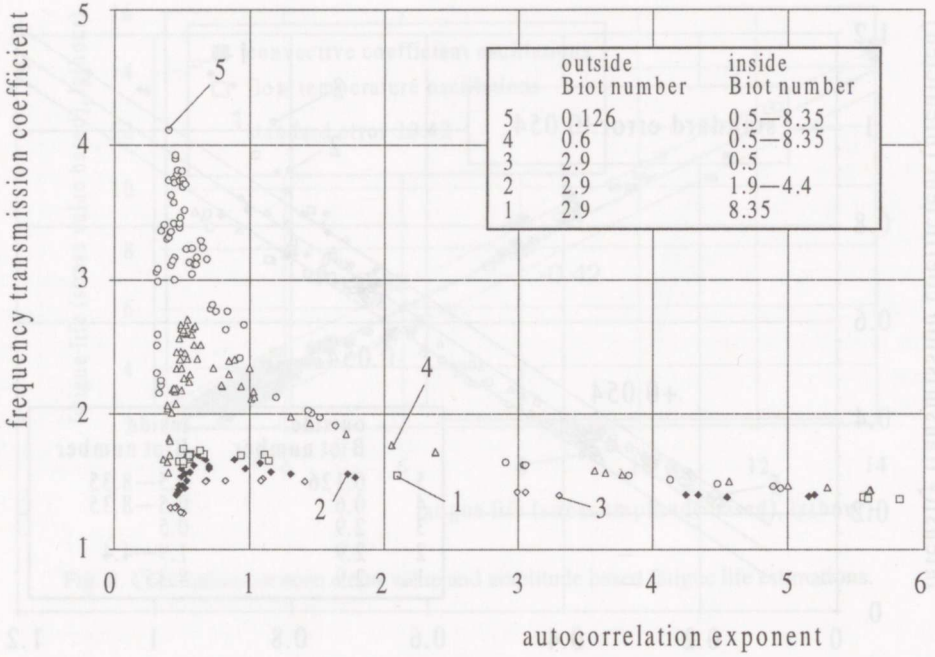

Fig. 11. Dependence of the frequency transmission coefficient on the autocorrelation exponent.

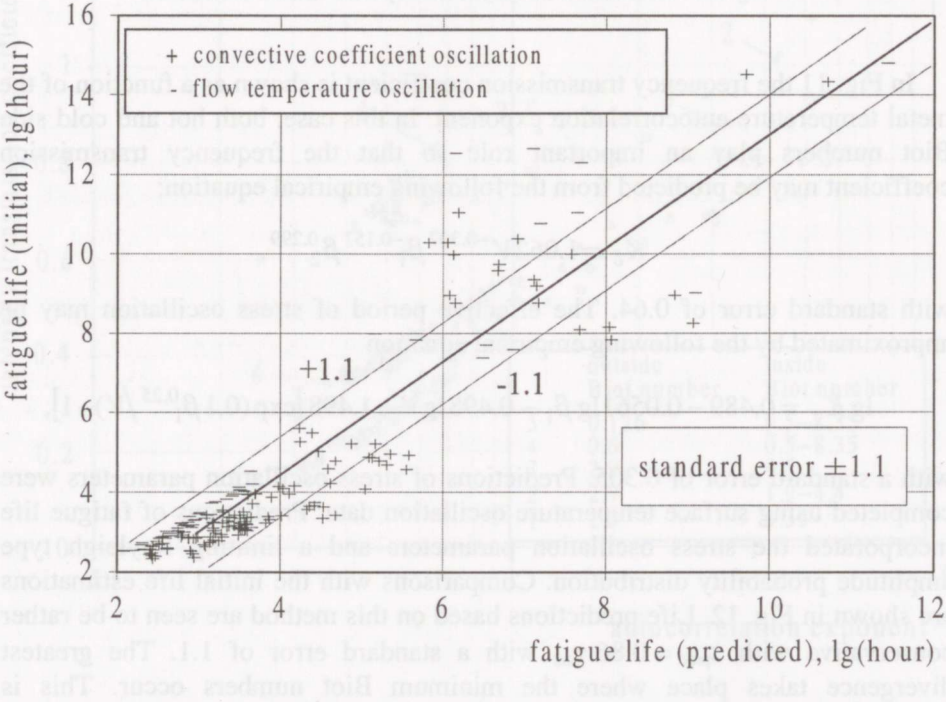

Fig. 12. Prediction of fatigue life on the basis of metal temperature oscillation parameter.

small Biot numbers and, consequently, small stress amplitudes, i.e., less than the fatigue endurance limit σ_{-1}, the fatigue curves have a very slight inclination (at $m = 30$) so that even very small divergences in predicted stress amplitudes lead to significant divergences in the life predictions.

5. CONCLUSIONS

1. Superimposed low frequency fluctuations significantly increase temperature and stress oscillation amplitudes while amplitudes of the convective coefficients and flow inlet temperature remain constant. As the stress amplitudes increase, the fatigue life decreases significantly.

2. An increase in the effect of superimposed low frequency fluctuations, characterized by a decreasing relative rivulet length in the range from one to zero, changes the nature of temperature and stress oscillations. At a relative rivulet length about one, the fluctuations follow a normal random process with statistical parameters showing a Gaussian or Rayleigh amplitude distribution, diminishing with increasing low frequency fluctuations. The autocorrelation exponent V may be taken as a quantitative indicator of the variation.

3. Differences between stress value and amplitude based fatigue life estimates are negligible despite significant differences in the respective basic stress and loading parameters.

4. The oscillation intensity and frequency transmission coefficients have been found to adequately characterize stress and loading parameters induced by temperature or convective coefficient oscillations. The variation in the predicted life estimates does not exceed 40% for all the cases investigated.

REFERENCES

1. Sudakov, A. and Trofimov, A. *Temperature Oscillations and Fatigue Life of Energy Equipment Elements*. Energoatomizdat, Leningrad, 1989 (in Russian).
2. Chiang, T., France, D. M., and Bump, T. R. Calculation of tube degradation induced by dryout instability in sodium-heated steam generators. *Nucl. Eng. Des.*, 1977, **41**, 2, 181–191.
3. Kao, T. T., Cho, S. M., and Pai, D. H. Thermal modelling of steam generator tubing under CHF-induced temperature oscillations. *Int. J. Heat Mass Transf.*, 1982, **25**, 6, 781–790.
4. Manson, S. S. and Halford, G. R. Re-examination of cumulative fatigue damage analysis – an engineering perspective. *Eng. Fract. Mech.*, 1986, **25**, 5/6, 539–571.
5. Klevtsov, I. and Tugov, A. Remaining life estimation for materials probabilistic stress oscillations using loading process's statistical parameters. *Trans. Tallinn Technical Univ.*, 1989, **692**, 57–67.
6. Klevtsov, I. and Kaar, H. Calculation of once-through steam generator tube fatigue life in transition boiling zone. *Recent Advances in Heat Transfer*. Elsevier, Amsterdam, 1992, 1241–1251.
7. Collins, J. A. *Failure of Materials in Mechanical Design. Analysis, Prediction, Prevention*. Wiley, New York, 1981.
8. Bendat, J. S. and Piersol, A. G. *Random Data: Analysis and Measurement Procedure*. Wiley, New York, 1971.

METALLI TSÜKLILISE VÄSIMUSE MÄÄRAMINE JUHUSLIKULT MUUTUVA PINGE KORRAL

Ivan KLEVTSOV ja Roger CRANE

Pulsatsiooni tingimustes töötava toru väsimuse (see väljendub esimeste mikropragude tekkes) täpsemaks määramiseks on välja töötatud arvutiprogrammid metalli pingeoleku modelleerimiseks. On hinnatud otsevoolu aurugeneraatori ja soojusvaheti torude väsimust. Esimesel juhul seati piirtingimused juhuslikult pulseerivale soojusülekandele ja teisel juhul juhuslikult muutuvale temperatuurile. Sellest lähtuvalt arvutati pinged ja temperatuuri jaotus toru seinas. Saadud andmeid analüüsiti statistiliselt, et hinnata parameetreid, mille alusel määrata elemendi väsimus.